

Solitons Bound to Heavy Mesons

Yongseok Oh¹

*Institut für Theoretische Physik, Physik Department, Technische Universität München, D-85747
Garching, Germany*

Byung-Yoon Park²

Department of Physics, Chungnam National University, Daejeon 305-764, Korea

ABSTRACT

We improve the bound state approach of the Skyrme model applied to the heavy baryons by adopting a static heavy meson picture where the soliton moves around the fixed heavy meson. This allows to take into account the center of mass corrections in a more consistent way. The bound state masses so obtained are comparable to the experimentally observed Λ_c and Λ_c^* masses. A loosely bound state of a soliton with an antistrange heavy meson is found, which leaves a possibility of the nonstrange pentaquark baryon(s).

PACS number(s): 12.39.Dc, 12.39.Hg, 14.20.Lq

¹e-mail address : yoh@physik.tu-muenchen.de

²e-mail address : bypark@nsphys.chungnam.ac.kr

1 Introduction

In the Skyrme model, heavy baryons containing a single charm or bottom quark can be described by bound states of soliton and the heavy meson of the corresponding heavy flavor [1–9]. It was first developed to describe strange hyperons [10] and was extensively applied to heavy baryons by Rho, Riska and Scoccola [1], for which the SU(3) symmetric Lagrangian was strongly modified to incorporate large flavor-symmetry breaking. Although qualitatively successful, because of the lack of the heavy quark symmetry in their Lagrangian, the resulting heavy baryon spectra could not be consistent with the required symmetry. Later, Jenkins, Manohar and Wise [2] have resolved this problem by adopting a proper heavy-meson effective Lagrangian [11] that incorporates both the chiral symmetry and the heavy quark symmetry explicitly. Based on the model Lagrangian of Ref. [11], we have carefully examined this picture to study the heavy baryon states with higher spin [12] and also to study nonstrange pentaquark exotic baryons [13]³.

These works started out in the large N_c (number of color) and large m_Q (heavy quark mass) limit where the soliton and the heavy mesons are infinitely heavy so that they sit on the top of each other. Such a simple picture is not good enough to describe quantitatively the real heavy baryons, especially the excited states. In a series of papers [15, 16], we have tried to improve the model by incorporating the finite mass effects of the heavy mesons. We adopted an effective Lagrangian [17] constructed for the heavy mesons of finite mass and solved exactly the equations of motion of the heavy mesons derived from it. The results are comparable to the quark model calculations in the charm and/or bottom sector.

However, we have worked in the conventional soliton-fixed frame by taking infinite N_c limit but with finite m_Q . It raises the conceptual problem of ‘the tail wagging the dog’ [1]. Actually such a problem has been present even in the bound state approach to the strange hyperons. Since the mass of the kaon is about one half of the soliton mass, a large center of mass correction is expected. In case of the bound state approach to heavy baryons, the situation is worse; the heavy meson is much heavier than the soliton — D (B) meson masses are around 2 GeV (5 GeV) whereas the soliton mass is about 1 GeV. Therefore it is obviously questionable that the former moves around the latter. A phenomenological consequence is that the heavy quark flavor symmetry appears broken much more than expected [16]. As a crude way of estimating the center of mass correction, the reduced mass of the heavy-meson–soliton system was used instead of the heavy meson mass [16, 18], which results in a quite different spectrum.

In the real world, however, since the heavy mesons are much heavier than the soliton, the soliton-fixed frame may not be a good starting point if one wants to treat any center of mass corrections in a perturbative way. It would be more reasonable to start from the opposite picture where the soliton moves in the heavy-meson-fixed frame, i.e., infinite m_Q limit but with finite N_c . Work along this direction was first developed in Ref. [4], where the interaction between the heavy meson and the soliton was approximated to that of the simple harmonic oscillator. The effect of the kinetic motion to the ground state energy is included through the zero point energy. In Ref. [19], the same harmonic approximation is adopted to describe the excited states Λ_Q^* . However, the crudeness of the approximate potential leads to the Λ_Q^* states lying high above the experimental observation.

In this paper, we improve the harmonic approximation of Refs. [4, 19] by obtaining the equation of motion for the soliton in a more realistic way. In the conventional soliton-fixed picture, the equations of motion for the heavy mesons have been easily derived from the given heavy meson effective Lagrangian after substituting the stationary hedgehog ansatz for the soliton configuration centered at the origin. On the contrary, in the picture of fixed heavy meson, we already have a known wavefunction of the heavy meson which should be localized at the origin. So the static hedgehog ansatz is necessarily modified to generate the kinetic motion of the soliton. For this purpose, we introduce the collective coordinates representing the translational motion of the soliton. The classical Lagrangian of

³For an extension of this idea to the NJL soliton model, see, for example, Ref. [14].

the collective coordinates is then obtained when the given effective Lagrangian density is integrated over the space with the heavy meson fields localized at the origin and the chiral field of the soliton configuration. Canonical quantization, then, leads to a nonrelativistic Schrödinger equation for the motion of the soliton interacting with the heavy meson sitting at the origin. This process is described in Sec. 2.

In Sec. 3, we compare the resulting equation of motion with that of the harmonic oscillator approximation. The Schrödinger equation is solved numerically to obtain the bound states. The model yields a few bound states of soliton and heavy mesons and the results are compared with the available experimental masses of Λ_c and Λ_c^* states. We also investigate the bound state(s) of the soliton to the antiflavored heavy mesons, which corresponds to the pentaquark ($\bar{Q}q^4$) exotic baryons. Section 4 contains a summary and conclusion and we provide detailed expressions in Appendices.

2 Soliton motion in the heavy meson fixed frame

We start from the heavy meson effective Lagrangian of leading order in $1/m_Q$ expansion [11], which reads

$$\mathcal{L} = \mathcal{L}_M + iv_\mu \text{Tr}[H(\partial^\mu + V^\mu)\bar{H}] + g_Q \text{Tr}(H\gamma^\mu\gamma_5 A_\mu\bar{H}), \quad (2.1a)$$

where \mathcal{L}_M is an $SU(2) \times SU(2)$ chiral Lagrangian governing the dynamics of the Goldstone bosons. For a simplicity, we will take the Skyrme model Lagrangian for \mathcal{L}_M ;

$$\mathcal{L}_M = \frac{f_\pi^2}{4} \text{Tr}(\partial_\mu U^\dagger \partial^\mu U) + \frac{1}{32e^2} \text{Tr}[U^\dagger \partial_\mu U, U^\dagger \partial_\nu U]^2, \quad (2.1b)$$

with the pion field represented by $U = \exp(i\boldsymbol{\tau} \cdot \boldsymbol{\pi}/f_\pi)$. The vector and axial-vector fields V_μ and A_μ are defined as

$$V_\mu = \frac{1}{2}(\xi^\dagger \partial_\mu \xi + \xi \partial_\mu \xi^\dagger), \quad (2.1c)$$

$$A_\mu = \frac{i}{2}(\xi^\dagger \partial_\mu \xi - \xi \partial_\mu \xi^\dagger), \quad (2.1d)$$

in terms of $\xi = \exp(i\boldsymbol{\tau} \cdot \boldsymbol{\pi}/2f_\pi)$. The heavy meson fields are combined into a 4×4 matrix field $H(x)$ as

$$H = \frac{1 + \not{v}}{2}(P_\mu^* \gamma^\mu - P \gamma_5) \quad \text{and} \quad \bar{H} = \gamma_0 H^\dagger \gamma_0, \quad (2.1e)$$

with the help of the standard Dirac matrices γ_μ and γ_5 . Here, P and P_μ^* are the heavy pseudoscalar and vector mesons moving with 4-velocity v_μ , respectively. This Lagrangian contains three physical constants, the pion decay constant f_π , the Skyrme parameter e and the coupling constant g_Q of heavy mesons. We will take them as free parameters varying around their empirical values ($f_\pi \sim 93$ MeV and $e \sim 4.8$) together with a nonrelativistic quark model prediction ($g_Q = -\frac{3}{4}$). One can easily check the invariance of the Lagrangian (2.1) under the $SU(2)_L \times SU(2)_R$ chiral transformation

$$\begin{aligned} U &\rightarrow LUR^\dagger \quad (\xi \rightarrow L\xi h^\dagger = h\xi R^\dagger), \\ H &\rightarrow Hh^\dagger. \end{aligned} \quad (2.1f)$$

In the conventional bound state approaches, the static soliton configuration centered at the origin $U_0(\mathbf{r}) = \exp[i\boldsymbol{\tau} \cdot \hat{\mathbf{r}}F(r)]$ is substituted into the Lagrangian and the resulting equations of motion for the heavy-flavored mesons (or kaons) moving in the static potentials arising from the soliton are solved to find the bound states. This ‘soliton–fixed’ picture supported from the large N_c arguments could be a good starting point for the strange baryons, which could be improved by proper center of mass corrections later. In case of the bound state approach to heavy baryons, however, the situation is quite

different. The observed heavy mesons D and D^* or B and B^* are definitely much heavier than the soliton. In this case, more reasonable starting point would be the heavy-meson–fixed picture, where the soliton moves around the heavy meson fixed at the origin and the corrections from the finite heavy meson mass could be included perturbatively.

In the heavy-meson–fixed frame, the spatial part of the heavy meson wavefunction is already determined by a well-localized function at origin such as $\delta^3(\mathbf{r})$. To generate the motion of the soliton, we substitute an ansatz [20]

$$U(\mathbf{r}, t) = U_0(\mathbf{r} - \mathbf{x}(t)), \quad (2.2)$$

into the Lagrangian for the soliton configuration with its center at $\mathbf{x}(t)$. Carrying out the integration over \mathbf{r} , we obtain the classical Lagrangian for the collective variables $\mathbf{x}(t)$ as⁴

$$L = \int d^3r \mathcal{L} = M_s + \frac{1}{2}M_s \mathbf{u}^2 - \frac{2v(x)}{x} \mathbf{u} \cdot (\mathbf{I}_h \times \mathbf{x}) - V_I, \quad (2.3a)$$

where

$$V_I = 2g_Q[a_1(x)\mathbf{S}_{\ell h} \cdot \mathbf{I}_h + a_2(x)\mathbf{S}_{\ell h} \cdot \hat{\mathbf{x}} \mathbf{I}_h \cdot \hat{\mathbf{x}}], \quad (2.3b)$$

and $\mathbf{u} = d\mathbf{x}/dt$ is the velocity of the soliton and M_s the soliton mass. (From now on, we will drop the trivial soliton mass term from the Lagrangian.) $\mathbf{S}_{\ell h}$ and \mathbf{I}_h are the light quark spin and isospin operator of the heavy mesons, respectively. The radial functionals $v(x)$, $a_1(x)$ and $a_2(x)$ are defined as

$$v(x) = \frac{\sin^2(F/2)}{x}, \quad a_1(x) = \frac{\sin F}{x} \quad \text{and} \quad a_2(x) = \frac{dF}{dx} - \frac{\sin F}{x}. \quad (2.3c)$$

The classical Hamiltonian is obtained by taking the Legendre transformation of the Lagrangian (2.3),

$$H_{\text{cl}} = \frac{1}{2M_s} \left\{ \mathbf{p}^2 + \frac{4v}{x} \mathbf{I}_h \cdot \mathbf{L} + 2v^2 \right\} + V_I(x), \quad (2.4)$$

with the conjugate momentum \mathbf{p} defined as

$$\mathbf{p} = \frac{\partial L}{\partial \mathbf{u}} = M_s \mathbf{u} - \frac{2v}{x} (\mathbf{I}_h \times \mathbf{x}). \quad (2.5)$$

Quantization of this collective motion leads us to the Schrödinger equation in the form of [4]

$$\left\{ -\frac{1}{2M_s} \nabla^2 + \frac{1}{2M_s} \left[\frac{4v}{x} \mathbf{I}_h \cdot \mathbf{L} + 2v^2 \right] + V_I \right\} \Psi_n(\mathbf{x}) = \varepsilon_n \Psi_n(\mathbf{x}). \quad (2.6)$$

The wavefunction $\Psi(\mathbf{x})$ depends not only on the collective coordinates \mathbf{x} but also on the light-quark spin $s_{\ell h}$ and the isospin i_h of the heavy mesons.

Since the Hamiltonian commutes only with the ‘light-quark grand spin’ operator defined by $\mathbf{K}_\ell = \mathbf{L} + \mathbf{S}_{\ell h} + \mathbf{I}_h$, the eigenstates can be classified by the corresponding quantum numbers (k_ℓ, m) and the wavefunction can be written as

$$\Psi(\mathbf{x}) = \sum_i \psi_i(x) \langle \hat{\mathbf{x}} | k_\ell, m \rangle_i, \quad (2.7)$$

where the summation i runs over the possible ways of combining the grand spin eigenstates $\langle \hat{\mathbf{x}} | k_\ell, m \rangle$ from orbital angular momentum basis $Y_{\ell, m_\ell}(\hat{\mathbf{x}})$, light-quark spin basis $|s_{\ell h} = \frac{1}{2}, \pm \frac{1}{2}\rangle$ and the isospin basis $|i_h = \frac{1}{2}, \pm \frac{1}{2}\rangle$ of the heavy mesons.

For a given $k_\ell (\neq 0)$, there are four possible eigenstates (see Appendix A) and, because of their different parity, only two states are mixed for a given parity. The wavefunction, then, can be written explicitly as

$$\Psi(\mathbf{x}) = \psi_1(x) \langle \hat{\mathbf{x}} | k_\ell, m \rangle_1 + \psi_2(x) \langle \hat{\mathbf{x}} | k_\ell, m \rangle_2, \quad (2.8)$$

⁴We treat the soliton motion nonrelativistically.

for the states of parity $\pi = -(-1)^{k_\ell}$, and

$$\Psi(\mathbf{x}) = \psi_3(x) \langle \hat{\mathbf{x}} | k_\ell, m \rangle_3 + \psi_4(x) \langle \hat{\mathbf{x}} | k_\ell, m \rangle_4, \quad (2.9)$$

for the states of parity $\pi = +(-1)^{k_\ell}$ including the intrinsic parity of heavy mesons.

Then, the Schrödinger equation (2.6) is reduced to coupled ordinary differential equations for the radial functions $\psi_i(x)$ as

$$\left\{ -\frac{1}{2M_s} \left[\frac{d^2}{dx^2} + \frac{2}{x} \frac{d}{dx} \right] \mathbf{1}_2 + V_{\text{eff}} \right\} \psi_n(x) = \varepsilon_n \psi_n(x), \quad (2.10a)$$

with the 2×2 unit matrix $\mathbf{1}_2$, where V_{eff} is in the form of 2×2 matrix

$$V_{\text{eff}}(x) = \begin{pmatrix} V_{11} & V_{12} \\ V_{21} & V_{22} \end{pmatrix} \text{ or } \begin{pmatrix} V_{33} & V_{34} \\ V_{43} & V_{44} \end{pmatrix}, \quad (2.10b)$$

and the corresponding radial function $\psi(x)$ is

$$\psi(x) = \begin{pmatrix} \psi_1(x) \\ \psi_2(x) \end{pmatrix} \text{ or } \begin{pmatrix} \psi_3(x) \\ \psi_4(x) \end{pmatrix}. \quad (2.10c)$$

The explicit expressions for the potentials V_{ij} can be found in Appendix A.

3 Bound states of soliton

Before solving the Schrödinger equation numerically, let us compare Eq. (2.10) with the harmonic approximation of Refs. [4, 19]. By making use of the fact that the soliton function $F(x)$ behaves near its center as

$$F(x) = \pi + F'(0)x + \frac{1}{6}F'''(0)x^3 + O(x^4), \quad (3.1)$$

we can expand the radial functionals of Eq. (2.3c) as

$$\begin{aligned} v(x) &= \frac{1}{x} - \frac{1}{4}[F'(0)]^2 x + O(x^3), \\ a_1(x) &= -F'(0) - \frac{1}{6}\{F'''(0) - [F'(0)]^3\}x^2 + O(x^3), \\ a_2(x) &= 2F'(0) + \frac{1}{6}\{4F'''(0) - [F'(0)]^3\}x^2 + O(x^3). \end{aligned} \quad (3.2)$$

In the extreme limit of $N_c \rightarrow \infty$, the soliton is also infinitely heavy so that it sits on the top of the heavy mesons. The binding energy of the system is the value of the potentials at the origin. Neglecting the centrifugal energy coming from the kinetic motion of the soliton, we obtain

$$\begin{aligned} \tilde{V}_{\text{eff}}(0) &= \frac{1}{2}g_Q F'(0) \begin{pmatrix} 1 & 0 \\ 0 & 1 \end{pmatrix}, \\ \tilde{V}_{\text{eff}}(0) &= -\frac{g_Q F'(0)}{2(2k_\ell + 1)} \begin{pmatrix} 2k_\ell + 3 & -4\sqrt{k_\ell(k_\ell + 1)} \\ -4\sqrt{k_\ell(k_\ell + 1)} & 2k_\ell - 1 \end{pmatrix}, \end{aligned} \quad (3.3)$$

for $\pi = -(-1)^{k_\ell}$ states and $\pi = +(-1)^{k_\ell}$ states, respectively. (In order to distinguish the potentials obtained with no centrifugal energy, we use the tilde on V .) Diagonalization of those potential matrices yields the results of Refs. [12, 13]; that is, degenerate heavy-meson-soliton bound states with binding energy $-\frac{3}{2}g_Q F'(0)$ and antiflavored-heavy-meson-soliton bound states with binding energy $-\frac{1}{2}g_Q F'(0)$. These degeneracies are of course the artifacts of ignoring the kinetic motion, especially, the centrifugal energy.

Table 1: V_0 and κ evaluated with conventional Skyrme model parameters. Energies are given in MeV unit and κ in MeV^3 unit.

Set	f_π	e	g_Q	M_s	V_0	κ	E_b	E_e
(I)	64.5	5.45	-0.75	867	-791	$(575)^3$	-88	468
(II)	64.5	5.45	-1.00	867	-1055	$(632)^3$	-246	540
(III)	93.0	4.82	-0.75	1105	-1009	$(733)^3$	-113	597
(IV)	93.0	4.82	-1.00	1105	-1345	$(807)^3$	-311	690
Expt.	93.0	-	-	867	-1095	$(437)^3$	-630	310

In case of $k_\ell^\pi = 0^+$, we have only one state $\langle \hat{x} | k_\ell = 0, 0 \rangle_3$. Although this state is made of $\ell = 1$ angular momentum basis, the associated singularity in the centrifugal energy is canceled by the same one of $v(x)$ in the potential, and the resulting effective potential is finite at the origin. Consequently, it provides the lowest energy bound state, if any. If we take the harmonic approximation of Eq. (3.2), the potential energy can be written as

$$V_{33}(x) \approx V_0 + \frac{1}{2}\kappa x^2, \quad (3.4a)$$

where

$$V_0 = -\frac{3}{2}g_Q F'(0), \quad (3.4b)$$

$$\kappa = g_Q \left\{ \frac{1}{3}[F'(0)]^3 - \frac{5}{6}F'''(0) \right\}. \quad (3.4c)$$

In Table 1, we list the values of V_0 and κ obtained by using Eq. (3.4a) with conventional parameters of the Skyrme model.

In this harmonic approximation, the eigenstates can be easily obtained as

$$\varepsilon_n = V_0 + \sqrt{\frac{\kappa}{M_s}} \left(n + \frac{3}{2} \right), \quad (3.5)$$

where n is an even integer number. The lowest energy state of $n=0$ is the ground state which has a negative energy, which corresponds to the binding energy of the Λ_Q baryon. From Eq. (3.5), we can write the mass formula for $\Lambda_Q(\frac{1}{2}^+)$ baryons as

$$m_{\Lambda_Q} = m_N + m_H + V_0 + \sqrt{\frac{\kappa}{M_s}} \left(N + \frac{3}{2} \right), \quad (3.6)$$

where we have included the mass of the heavy mesons m_H and the nucleon mass m_N (soliton mass plus the energy from collective rotation). The kinetic motion of the soliton with finite mass is included through the zero point energy of $\frac{3}{2}\sqrt{\kappa/M_s}$. The artificial degeneracy in the model of $N_c, m_Q \rightarrow \infty$ is thus removed, while only the ground state is bound.

In Ref. [19], this harmonic approximation of the potential was straightforwardly extended to $k_\ell > 0$ states by simply adding the centrifugal energy. The tensor couplings of V_{12} (V_{34}) between the $|k_\ell, m\rangle_1$ and $|k_\ell, m\rangle_2$ states ($|k_\ell, m\rangle_3$ and $|k_\ell, m\rangle_4$ states) was not taken into account in this approximation. Then, the potential gives rise to an infinite tower of eigenenergies of Eq. (3.5) for any integer n . The first excited $k_\ell^\pi = 1^-$ states which is $\sqrt{\kappa/M_s}$ above the ground state could be interpreted as $\Lambda_Q^*(\frac{1}{2}^-)$ and $\Lambda_Q^*(\frac{3}{2}^-)$ states. In order to fit the observed masses of Λ_c (2285 MeV), $\Lambda_c^*(\frac{1}{2}^-)$ (2593 MeV) and $\Lambda_c^*(\frac{3}{2}^-)$ (2625 MeV) [21, 22], we need to have the binding energy E_b and the excitation energy E_e as

$$\begin{aligned} E_b &= V_0 + \frac{3}{2}\sqrt{\kappa/M_s} = -630 \text{ MeV}, \\ E_e &= \sqrt{\kappa/M_s} = 310 \text{ MeV}, \end{aligned} \quad (3.7)$$

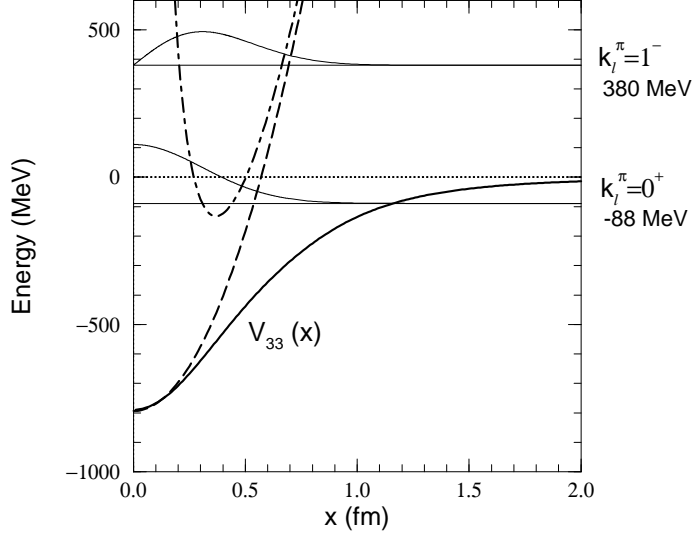


Figure 1: Potentials and wavefunctions in the harmonic oscillator approximation with the parameter set (I). The solid line is the exact form of V_{33} and the long dashed line is its harmonic approximation. The potential of $k_l^\pi = 1^-$ state including the centrifugal energy is given by the dot-dashed line. The corresponding wavefunctions are also presented.

which are regarded as the ‘experimental’ values in Table 1. As can be seen in Table 1, under the harmonic approximation, it is not easy to fit the experimental values by adjusting the parameters of the Skyrme model around their empirical values in a reasonable range, which was also pointed out in Ref. [18].

Shown in Fig. 1 is the harmonic approximation (long dashed line) of the potential $V_{33}(x)$ in comparison with the exact one (solid line). The dot-dashed curve is the effective potential in the harmonic approximation with the centrifugal energy $\ell_{\text{eff}}(\ell_{\text{eff}} + 1)/(2M_s x^2)$ with ($\ell_{\text{eff}} = 1$) included. The lowest energy levels of the corresponding harmonic potentials are explicitly presented with their wavefunctions in the parameter set (I). First of all, compared with the exact one, the approximate potential is too stiff. Because of this crudeness of the harmonic oscillator potential, the zero point fluctuation and the excitation energy become too large. This is crucial for the excited states whose wavefunctions are spread over a wide range. Consequently, the binding energy of the Λ_Q appears too small and the first excited Λ_Q^* state locates too high above the experimental observations for all the parameter sets adopted in Table 1.

Now, let us investigate the exact solutions. In Fig. 2, we present two $k_l^\pi = 0^+$ bound states and their wavefunctions obtained with the parameter set (I). Comparing with those of the harmonic approximation (Fig. 1), the exact wavefunctions are more expanded so that the eigenstates get more binding. In Fig. 3, solid lines are the potential energies $V_{ij}(i, j = 3, 4)$ for the $k_l^\pi = 1^-$ state. At a first glance, there does not appear any attractive part in each potential, with the exception of V_{44} which is however not strong enough to support a bound state. To understand the binding mechanism, we diagonalize the potential matrix at each position x :

$$S(x)V_{\text{eff}}S^\dagger(x) = \text{diag}(V^+, V^-), \quad (3.8)$$

where

$$V^\pm(x) = \frac{1}{2}[(V_{33} + V_{44}) \pm \sqrt{(V_{33} - V_{44})^2 + 4V_{34}^2}]. \quad (3.9)$$

These V^\pm are presented by dashed lines in Fig. 3. The off-diagonal potential V_{34} pushes down V_{44} so

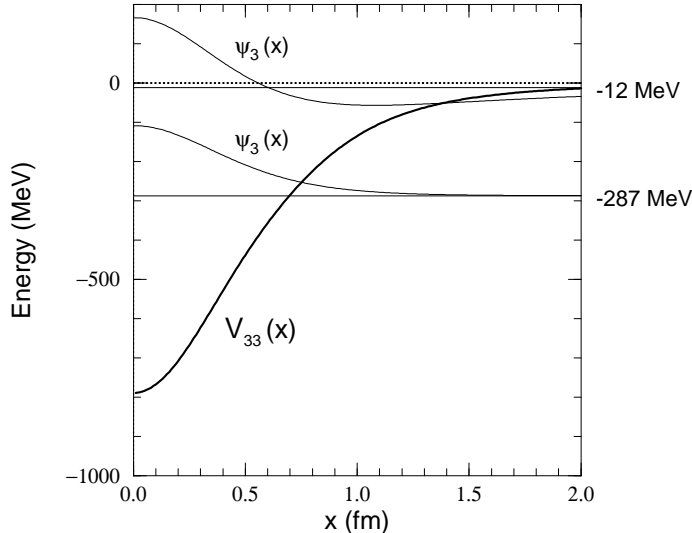


Figure 2: Solutions for the $k_\ell^\pi = 0^+$ bound states with the parameter set (I). Thick solid line is the potential V_{33} and the solid lines are the wavefunctions of the ground and radially excited states.

Table 2: Numerical results on the bound states. Energies are given in MeV unit.

(n, k_ℓ^π)	Set I	Set II	Set III	Set IV	Exp.
$(0, 0^+)$	-287	-461	-366	-588	-610
$(1, 0^+)$	-12	-62	-15	-79	—
$(0, 1^-)$	-89	-196	-113	-250	-320
$(0, 1^+)^*$	-17	-54	-21	-69	—

* bound state of soliton to ant flavored heavy meson

that it becomes sufficiently attractive to support a bound state. Of course, one should *not* use one of the diagonalized potentials, V^+ or V^- , to obtain the eigenstates of the equation of motion because the similarity transformation matrix $S(x)$ of Eq. (3.8) is local. Instead, one should follow the general procedure to solve the coupled equations as described in Appendix B. The resulting bound state is shown in the inner box of Fig. 3 with its wave functions $\psi_3(x)$ and $\psi_4(x)$ (solid lines). There, V^- is drawn only as a guiding line.

We summarize our numerical results in Table 2. We list the bound states of the model with four different parameter sets (I)–(IV). In each case, we could find two bound states in the $k_\ell^\pi = 0^+$ channel and one in the 1^- channel. This should be contrasted with the results of the soliton-fixed frame of Ref. [16], where many bound states appear as we increase the heavy meson mass. The coupling constant predicted by the nonrelativistic quark model ($|g_Q| = \frac{3}{4}$) yields too small binding energies compared with the experimental values. By increasing its magnitude to 1, which may represent the role of light vector mesons [18], we could obtain reasonable values. Comparing with the parameter set (I) and (II) with $f_\pi = 64.5$ MeV and $e = 5.45$, set (III) and (IV) of $f_\pi = 93$ MeV and $e = 4.82$ result in more strongly bound states. It is mainly due to the different shapes of the potentials and partly due to the heavier soliton mass ($M_s = 1105$ MeV) of the latter which slightly exceeds the required mass 867 MeV to fit the nucleon mass. In adopting these parameter sets, we account for the Casimir energy [23] that will reduce down the final soliton mass.

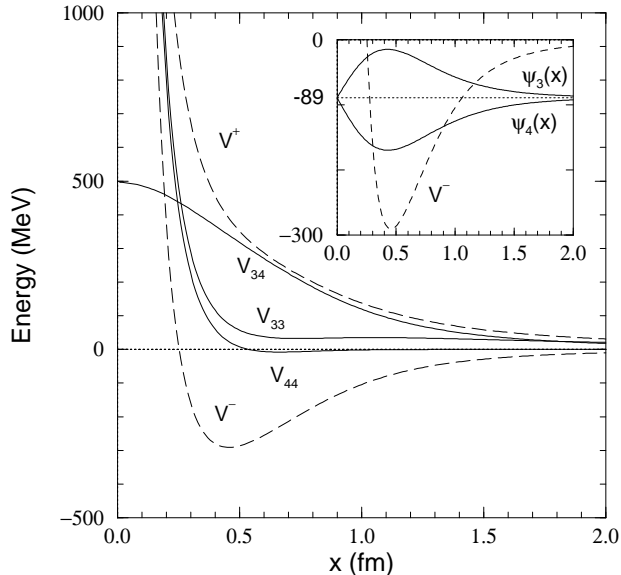


Figure 3: Solutions for the $k_\ell^\pi = 1^-$ bound states with parameter set (I). The solid lines are potentials V_{ij} ($i, j = 3, 4$) and the dashed lines are V^\pm . The wavefunctions are given in the inner box with V^- .

The last line of Table 2 is the result for soliton bound state to the antinflavored heavy meson, which corresponds to the pentaquark ($\bar{Q}q^4$) exotic baryon in the quark model where $q = u, d$ quarks. It can be searched simply by changing the sign of the coupling constant g_Q [13, 24]. We could find only one bound state in the $k_\ell^\pi = 1^+$ channel. Shown in Fig. 4 are the potentials $V_{ij}(i, j = 1, 2)$ for the soliton–antinflavored-heavy-meson interactions (solid lines), the diagonalized one as in Fig. 3 (dashed lines) and the wavefunctions $\psi_1(x)$ and $\psi_2(x)$ of the bound state (inner box). In case of the nonrelativistic quark model value of g_Q , the state is bound too weakly to survive after the $1/m_Q$ corrections. However, with a coupling constant $|g_Q| \sim 1$ which yields reasonable soliton–heavy-meson bound states, the binding energy of the bound state of soliton and antinflavored-heavy-meson is somewhat large and it still leaves a possibility of loosely bound *nonstrange* pentaquark baryons.

4 Summary and Conclusion

In this paper, we have carried out the bound state approach of the Skyrme model to heavy baryons in a more realistic way. We obtain the bound states of the soliton and heavy meson in the fixed heavy-meson picture. It improves the harmonic approximation of Refs. [4, 19] by deriving the soliton–heavy-meson interacting potential in a more consistent way from a given effective Lagrangian. First we introduce the collective coordinates for the motion of the soliton. Then, the classical Lagrangian for these coordinates is obtained by carrying out the integral over the space with localized heavy meson fields. The nonrelativistic Schrödinger equation is obtained by quantizing the motion. The resulting bound states have larger binding energies than in the harmonic oscillator approximation. Apart from the ground state with $k_\ell^\pi = 0^+$, we could find the first excited state with negative parity in the $k_\ell^\pi = 1^-$ channel. With the value of $g_Q \sim 1$, which is slightly larger than the nonrelativistic quark model prediction, those resulting bound states are comparable to the experimentally observed $\Lambda_c(\frac{1}{2}^+)$ and $\Lambda_c^*(\frac{1}{2}^-, \frac{3}{2}^-)$ states.

This work also improves the work of Refs. [16] where the bound state approach was carried out in the conventional soliton-fixed picture. In this approach the heavy quark flavor symmetry is rather strongly broken as expected. Since the $1/m_Q$ order terms are not included in the Lagrangian, the

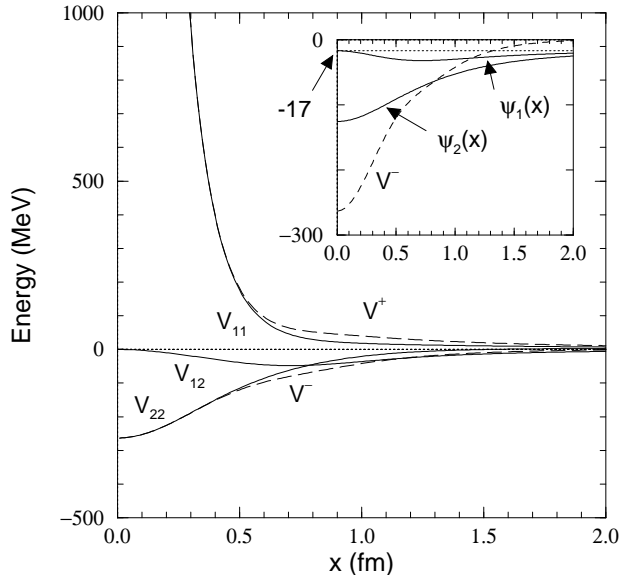


Figure 4: Solutions for the $k_\ell^\pi = 1^+$ soliton-antiflavored-heavy-meson bound states with the parameter set (I). The solid lines are potentials V_{ij} ($i, j = 1, 2$) and the dashed lines are V^\pm . The wavefunctions are given in the inner box with V^- .

obtained bound states do not depend on the flavor of the heavy mesons at that level of approximation. If one turns on the $1/m_Q$ corrections, this degeneracy will be removed as much as the heavy flavor is broken by the $1/m_Q$ order terms in the Lagrangian.

We have obtained just those bound states which are eigenstates of the light-quark grand spin operator. They could be naively compared with the $\Lambda_Q(\frac{1}{2}^+)$ and $\Lambda_Q^*(\frac{1}{2}^-, \frac{3}{2}^-)$ baryons. However, in order to provide those bound states with the correct quantum numbers such as spin and isospin, we have to quantize the zero modes of the bound states under the SU(2) rotation in isospin space. This procedure will enable us to check the model by comparing the results with the other observed heavy baryon states such as Σ_Q and Σ_Q^* [21, 25]. Work in this direction is in progress and will be reported elsewhere [26].

Acknowledgements

We are grateful to D.-P. Min and M. Rho for useful discussions and to W. Weise for careful reading of the manuscript with useful comments. One of us (Y.O.) thanks the Alexander von Humboldt Foundation for financial support. This work was supported in part by the Korea Science and Engineering Foundation through the SRC program.

A Matrix elements in k_ℓ basis

In this Appendix, we give the explicit expressions for the potential V_{ij} of Eq. (2.10).

The light-quark grand spin operator is defined as

$$\mathbf{K}_\ell = \mathbf{L} + \mathbf{I}_h + \mathbf{S}_{\ell h}, \quad (\text{A.1})$$

where \mathbf{I}_h and $\mathbf{S}_{\ell h}$ are the isospin and light-quark spin operators of the heavy mesons and \mathbf{L} is the orbital angular momentum operator of the soliton. It should be distinguished from the grand spin

Table 3: Four $\langle \hat{\mathbf{x}} | k_\ell m \rangle$ eigenstates for a given k_ℓ .

parity $\pi = -(-1)^{k_\ell}$			parity $\pi = +(-1)^{k_\ell}$		
state	ℓ_i	λ_i	state	ℓ_i	λ_i
$\langle \hat{\mathbf{x}} k_\ell, m \rangle_1$	$\lambda_i - \frac{1}{2}$	$k_\ell + \frac{1}{2}$	$\langle \hat{\mathbf{x}} k_\ell, m \rangle_3$	$\lambda_i + \frac{1}{2}$	$k_\ell + \frac{1}{2}$
$\langle \hat{\mathbf{x}} k_\ell, m \rangle_2$	$\lambda_i + \frac{1}{2}$	$k_\ell - \frac{1}{2}$	$\langle \hat{\mathbf{x}} k_\ell, m \rangle_4$	$\lambda_i - \frac{1}{2}$	$k_\ell - \frac{1}{2}$

operator \mathbf{K} that is the sum of the orbital angular momentum and all kinds of the spin or isospin of the particles in the model. Note that in the definition of the operator \mathbf{K}_ℓ only the angular momentum operators of the light degrees of freedom are included.

The eigenstates of the light-quark grand spin operator can be obtained by linear combinations of direct product of the eigenstates of each angular momentum operator in its definition:

$$\langle \hat{\mathbf{x}} | k_\ell, m \rangle_i = \sum_{m_t, m_s} (\ell_i m_\ell \frac{1}{2} m_t | \lambda_i m_\lambda) (\lambda_i m_\lambda \frac{1}{2} m_s | k_\ell m) Y_{\ell_i m_\ell}(\hat{\mathbf{x}}) | \frac{1}{2} m_t \rangle_t | \frac{1}{2} m_s \rangle_s, \quad (\text{A.2})$$

with the help of the Clebsch-Gordan coefficients [27]. Here, we first combine \mathbf{L} and \mathbf{I}_h (λ and m_λ are the corresponding quantum numbers of the eigenstates of $\mathbf{\Lambda} \equiv \mathbf{L} + \mathbf{I}_h$), and then combine the light-quark spin $\mathbf{S}_{\ell h}$. For a given $k_\ell (> 0)$, there come out four eigenstates as listed in Table 3. In case of $k_\ell = 0$, there can be only two states $\langle \hat{\mathbf{x}} | k_\ell, m \rangle_{1,3}$. In evaluating the total parity of the states as in Table 3, the negative intrinsic parity of the heavy mesons is taken into account.

To obtain the potentials $V_{ij}(i, j=1,2 \text{ or } 3,4)$ of Eq. (2.10), we need to evaluate the expectation values of the operators, $\mathbf{I}_h \cdot \mathbf{L}$, $\mathbf{I}_h \cdot \mathbf{S}_{\ell h}$ and $(\mathbf{I}_h \cdot \hat{\mathbf{x}})(\mathbf{S}_{\ell h} \cdot \hat{\mathbf{x}})$, with respect to the eigenstates $|k_\ell, m\rangle_i (i=1,2 \text{ or } 3,4)$. The first one is simple to evaluate the expectation values, since it can be rewritten as

$$\mathbf{I}_h \cdot \mathbf{L} = \frac{1}{2}(\mathbf{\Lambda}^2 - \mathbf{L}^2 - \mathbf{I}_h^2) = \begin{cases} \ell/2, & \text{if } \lambda = \ell + \frac{1}{2}, \\ -(\ell+1)/2, & \text{if } \lambda = \ell - \frac{1}{2}. \end{cases} \quad (\text{A.3})$$

Thus, it is trivial to obtain ${}_i \langle \mathbf{I}_h \cdot \mathbf{L} \rangle_j$ as

i, j	1	2	i, j	3	4
1	$\frac{1}{2}k_\ell$	0	3	$-\frac{1}{2}(k_\ell+2)$	0
2	0	$-\frac{1}{2}(k_\ell+1)$	4	0	$\frac{1}{2}(k_\ell-1)$

(A.4)

The expectation values of the operator $\mathbf{I}_h \cdot \mathbf{S}_{\ell h}$ can have a simpler form if we obtained the eigenstates of the operator \mathbf{K}_ℓ in another way; that is, by combining $\mathbf{S}_{\ell h}$ and \mathbf{I}_h first ($\mathbf{\Sigma}_\ell \equiv \mathbf{I}_h + \mathbf{S}_{\ell h}$ with the quantum numbers σ and m_σ), and then with \mathbf{L} . Let $|\ell, \sigma; k_\ell, m\rangle$ be such a state. Then, the eigenstates $|k_\ell, m\rangle_i$ can be related to the eigenstates $|\ell, \sigma; k_\ell, m\rangle$ by the Racah coefficients as

$$\begin{aligned} |k_\ell, m\rangle_1 &= \sqrt{\frac{k_\ell+1}{2k_\ell+1}} |\ell = k_\ell, \sigma = 0; k_\ell, m\rangle + \sqrt{\frac{k_\ell}{2k_\ell+1}} |\ell = k_\ell, \sigma = 1; k_\ell, m\rangle, \\ |k_\ell, m\rangle_2 &= -\sqrt{\frac{k_\ell}{2k_\ell+1}} |\ell = k_\ell, \sigma = 0; k_\ell, m\rangle + \sqrt{\frac{k_\ell+1}{2k_\ell+1}} |\ell = k_\ell, \sigma = 1; k_\ell, m\rangle, \\ |k_\ell, m\rangle_3 &= |\ell = k_\ell + 1, \sigma = 1; k_\ell, m\rangle, \\ |k_\ell, m\rangle_4 &= |\ell = k_\ell - 1, \sigma = 1; k_\ell, m\rangle. \end{aligned} \quad (\text{A.5})$$

By using the identity

$$\mathbf{I}_h \cdot \mathbf{S}_{\ell h} = \frac{1}{2}(\mathbf{\Sigma}_\ell^2 - \frac{3}{2}), \quad (\text{A.6})$$

we can obtain ${}_i\langle \mathbf{I}_h \cdot \mathbf{S}_{\ell h} \rangle_j$ as

$$\begin{array}{c|c|c}
i, j & 1 & 2 \\
\hline
1 & \frac{2k_\ell + 3}{4(2k_\ell + 1)} & \frac{\sqrt{k_\ell(k_\ell + 1)}}{2k_\ell + 1} \\
\hline
2 & \frac{\sqrt{k_\ell(k_\ell + 1)}}{2k_\ell + 1} & -\frac{2k_\ell - 1}{4(2k_\ell + 1)}
\end{array}
\quad
\begin{array}{c|c|c}
i, j & 3 & 4 \\
\hline
3 & \frac{1}{4} & 0 \\
\hline
4 & 0 & \frac{1}{4}
\end{array}
\tag{A.7}$$

Subtracting $\frac{1}{3}(\mathbf{I}_h \cdot \mathbf{S}_{\ell h})$, the third operator can be expressed in a tensor operator form of

$$\mathcal{O}_T \equiv (\mathbf{I}_h \cdot \hat{\mathbf{x}})(\mathbf{S}_{\ell h} \cdot \hat{\mathbf{x}}) - \frac{1}{3}(\mathbf{I}_h \cdot \mathbf{S}_{\ell h}). \tag{A.8}$$

By rewriting it as

$$\mathcal{O}_T = 2(\mathbf{I}_h \cdot \hat{\mathbf{x}})(\mathbf{I}_h \cdot \mathbf{S}_{\ell h})(\mathbf{I}_h \cdot \hat{\mathbf{x}}) + \frac{1}{6}(\mathbf{I}_h \cdot \mathbf{S}_{\ell h}), \tag{A.9}$$

which enables us to use the relations $2(\mathbf{I}_h \cdot \hat{\mathbf{x}})|k_\ell, m\rangle_i = -|k_\ell, m\rangle_{i+2}$ ($i=1,2$), we obtain ${}_i\langle \mathcal{O}_T \rangle_j$ as

$$\begin{array}{c|c|c}
i, j & 1 & 2 \\
\hline
1 & \frac{k_\ell}{6(2k_\ell + 1)} & \frac{\sqrt{k_\ell(k_\ell + 1)}}{6(2k_\ell + 1)} \\
\hline
2 & \frac{\sqrt{k_\ell(k_\ell + 1)}}{6(2k_\ell + 1)} & \frac{k_\ell + 1}{6(2k_\ell + 1)}
\end{array}
\quad
\begin{array}{c|c|c}
i, j & 3 & 4 \\
\hline
3 & -\frac{k_\ell + 2}{6(2k_\ell + 1)} & \frac{\sqrt{k_\ell(k_\ell + 1)}}{2(2k_\ell + 1)} \\
\hline
2 & \frac{\sqrt{k_\ell(k_\ell + 1)}}{2(2k_\ell + 1)} & -\frac{k_\ell - 1}{6(2k_\ell + 1)}
\end{array}
\tag{A.10}$$

Finally, we obtain V_{ij} ($i, j=1,2$ or $3,4$) as

$$\begin{aligned}
V_{11} &= V_r + V_{\text{cent}} + \frac{k_\ell}{2}V_{IL} - \frac{2k_\ell + 3}{4(2k_\ell + 1)}V_{IS} + \frac{k_\ell}{6(2k_\ell + 1)}V_T, \\
V_{12}(= V_{21}) &= \frac{\sqrt{k_\ell(k_\ell + 1)}}{2k_\ell + 1}V_{IS} + \frac{\sqrt{k_\ell(k_\ell + 1)}}{6(2k_\ell + 1)}V_T, \\
V_{22} &= V_r + V_{\text{cent}} - \frac{k_\ell + 1}{2}V_{IL} - \frac{2k_\ell - 1}{4(2k_\ell + 1)}V_{IS} + \frac{k_\ell + 1}{6(2k_\ell + 1)}V_T, \\
V_{33} &= V_r + V_{\text{cent}} - \frac{k_\ell + 2}{2}V_{IL} + \frac{1}{4}V_{IS} - \frac{k_\ell + 2}{6(2k_\ell + 1)}V_T, \\
V_{34}(= V_{43}) &= \frac{\sqrt{k_\ell(k_\ell + 1)}}{2(2k_\ell + 1)}V_T, \\
V_{44} &= V_r + V_{\text{cent}} + \frac{k_\ell - 1}{2}V_{IL} + \frac{1}{4}V_{IS} - \frac{k_\ell - 1}{6(2k_\ell + 1)}V_T.
\end{aligned}
\tag{A.11}$$

where $V_r = v^2/M_s$, $V_{\text{cent}} = \ell(\ell + 1)/(2M_s x^2)$, $V_{IL} = 2v/(M_s x)$, $V_{IS} = 2g_Q(a_1 + \frac{1}{3}a_2)$ and $V_T = 2g_Q a_2$.

B Numerical Process

Here, we briefly describe the numerical process of finding the bound states. Equation (2.10) can be solved like any other eigenvalue problem. First, we find the asymptotic solutions near the origin and at large x . Except the $k_\ell = 0$ case where only one radial function ($\psi_1(x)$ or $\psi_3(x)$) is defined, we can find two independent solution sets. (See Table 4.) Taking those independent sets of asymptotic solutions as initial conditions, the differential equation can be solved numerically in the forward or backward direction of x . In this way, we can obtain 8 radial functions (2 independent radial functions \times 2 independent initial conditions \times integrated forward or backward direction of x). Let us distinguish those radial functions by using scripts $>$ (or $<$) and A (or B). For example, $\psi_{1,A}^>$ denotes the radial

Table 4: Two independent asymptotic solutions near the origin and at large x .

	$\pi = -(-1)^{k_\ell}$		$\pi = +(-1)^{k_\ell}$	
	near the origin	at large x	near the origin	at large x
Sol. A	$\psi_1(x) \sim x^{k_\ell+1}$ $\psi_2(x) \sim 0$	$\psi_1(x) \sim e^{\sqrt{ \varepsilon_n x}}/x$ $\psi_2(x) \sim 0$	$\psi_3(x) \sim x^{k_\ell}$ $\psi_4(x) \sim 0$	$\psi_3(x) \sim e^{\sqrt{ \varepsilon_n x}}/x$ $\psi_4(x) \sim 0$
Sol. B	$\psi_1(x) \sim 0$ $\psi_2(x) \sim x^{k_\ell-1}$	$\psi_1(x) \sim 0$ $\psi_2(x) \sim e^{\sqrt{ \varepsilon_n x}}/x$	$\psi_3(x) \sim 0$ $\psi_4(x) \sim x^{k_\ell}$	$\psi_3(x) \sim 0$ $\psi_4(x) \sim e^{\sqrt{ \varepsilon_n x}}/x$

function obtained by starting from the asymptotic solution set A and solving the equation of motion in backward direction.

Then, a general solution that one can obtain by integrating the equation of motion in forward direction is expressed as

$$\begin{pmatrix} \psi_1^<(x) \\ \psi_2^<(x) \end{pmatrix} = \begin{pmatrix} \alpha_A \psi_{1,A}^< + \alpha_B \psi_{1,B}^< \\ \alpha_A \psi_{2,A}^< + \alpha_B \psi_{2,B}^< \end{pmatrix}, \quad (\text{B.1})$$

where $\alpha_{A,B}$ are arbitrary constants. Similarly, a general backward solution can be obtained as

$$\begin{pmatrix} \psi_1^>(x) \\ \psi_2^>(x) \end{pmatrix} = \begin{pmatrix} \beta_A \psi_{1,A}^> + \beta_B \psi_{1,B}^> \\ \beta_A \psi_{2,A}^> + \beta_B \psi_{2,B}^> \end{pmatrix}. \quad (\text{B.2})$$

At a proper intermediate position x_m , those wavefunctions should be matched in the way that the functions and their derivatives are continuous. This matching condition leads to a linear equation,

$$\begin{pmatrix} \psi_{1,A}^<(x_m) & \psi_{1,B}^<(x_m) & \psi_{1,A}^>(x_m) & \psi_{1,B}^>(x_m) \\ \psi_{2,A}^<(x_m) & \psi_{2,B}^<(x_m) & \psi_{2,A}^>(x_m) & \psi_{2,B}^>(x_m) \\ \psi_{1,A}^<'(x_m) & \psi_{1,B}^<'(x_m) & \psi_{1,A}^>'(x_m) & \psi_{1,B}^>'(x_m) \\ \psi_{2,A}^<'(x_m) & \psi_{2,B}^<'(x_m) & \psi_{2,A}^>'(x_m) & \psi_{2,B}^>'(x_m) \end{pmatrix} \begin{pmatrix} \alpha_A \\ \alpha_B \\ -\beta_A \\ -\beta_B \end{pmatrix} = 0. \quad (\text{B.3})$$

In order that it supports a nontrivial solution, the determinant of the matrix should vanish. Such a secular equation determines the eigenenergies. Once an eigenenergy is found, Eq. (B.3) can be solved for the ratios between the coefficients, $\alpha_{A,B}$ and $\beta_{A,B}$. Their absolute values can be fixed by normalizing the wavefunction.

In the special case of $k_\ell = 0$, there appears only one radial function, $\psi_1(x)$ or $\psi_3(x)$. The asymptotic solution of them is given as the solution set A in Table 2. In a similar way described above, one obtains the backward and forward solutions, $\psi_{1(3)}^>$ and $\psi_{1(3)}^<$, respectively. Simply by matching their logarithmic derivatives as

$$\left. \frac{\psi_{1(3)}^<' }{\psi_{1(3)}^<} \right|_{x=x_m} = \left. \frac{\psi_{1(3)}^>' }{\psi_{1(3)}^>} \right|_{x=x_m}, \quad (\text{B.4})$$

one can find the eigenstates.

References

- [1] M. Rho, D. O. Riska, and N. N. Scoccola, Phys. Lett. **B251** (1990) 597 ; Z. Phys. **A341** (1992) 343;
Y. Oh, D.-P. Min, M. Rho, and N. N. Scoccola, Nucl. Phys. **A534** (1991) 493.
- [2] E. Jenkins, A. V. Manohar, and M. B. Wise, Nucl. Phys. **B396** (1993) 27.

- [3] E. Jenkins and A. V. Manohar, Phys. Lett. **B294** (1992) 273;
Z. Guralnik, M. Luke, and A. V. Manohar, Nucl. Phys. **B390** (1993) 474.
- [4] E. Jenkins, A. V. Manohar, and M. B. Wise, Nucl. Phys. **B396** (1993) 38.
- [5] M. Nowak, M. Rho, and I. Zahed, Phys. Lett. **B303** (1993) 130;
H. K. Lee, M. A. Nowak, M. Rho, and I. Zahed, Ann. Phys. (N.Y.) **227** (1993) 175;
H. K. Lee and M. Rho, Phys. Rev. **D48** (1993) 2329.
- [6] K. S. Gupta, M. A. Momen, J. Schechter, and A. Subbaraman, Phys. Rev. **D47** (1993) 4835;
A. Momen, J. Schechter, and A. Subbaraman, Phys. Rev. **D49** (1994) 5970.
- [7] D.-P. Min, Y. Oh, B.-Y. Park, and M. Rho, Int. J. Mod. Phys. **E4** (1995) 47.
- [8] Y. Oh and B.-Y. Park, Mod. Phys. Lett. A **11** (1996) 653.
- [9] M. Harada, A. Qamar, F. Sannino, J. Schechter, and H. Weigel, Phys. Lett. **B390** (1997) 329.
- [10] C. G. Callan and I. Klebanov, Nucl. Phys. **B262** (1985) 222.
- [11] M. B. Wise, Phys. Rev. **D45** (1992) 2188.
- [12] Y. Oh, B.-Y. Park, and D.-P. Min, Phys. Rev. **D50** (1994) 3350.
- [13] Y. Oh, B.-Y. Park, and D.-P. Min, Phys. Lett. **B331** (1994) 362.
- [14] L. Gamberg, H. Weigel, U. Zückert, and H. Reinhardt, Phys. Rev. **D54** (1996) 5812.
- [15] Y. Oh, B.-Y. Park, and D.-P. Min, Phys. Rev. **D49** (1994) 4649.
- [16] Y. Oh and B.-Y. Park, Phys. Rev. **D51** (1995) 5016; Phys. Rev. **D53** (1996) 1605.
- [17] T.-M. Yan, H.-Y. Cheng, C.-Y. Cheung, G.-L. Lin, Y. C. Lin, and H.-L. Yu, Phys. Rev. **D46** (1992) 1148.
- [18] J. Schechter and A. Subbaraman, Phys. Rev. **D51** (1995) 2311;
J. Schechter, A. Subbaraman, S. Vaidya, and H. Weigel, Nucl. Phys. **A590** (1995) 655; (E) **A598** (1996) 583.
- [19] C.-K. Chow and M. B. Wise, Phys. Rev. **D50** (1994) 2135.
- [20] See for instance, E. Braaten, S.-M. Tse, and C. Willcox, Phys. Rev. **D34** (1986) 1482;
D. P. Cebula, A. Klein, and N. R. Walet, J. Phys. **G18** (1992) 499.
- [21] Particle Data Group, R. M. Barnett *et al.*, Phys. Rev. **D54** (1996) 1.
- [22] ARGUS Collaboration, H. Albrecht *et al.*, Phys. Lett. **B317** (1993) 227;
E687 Collaboration, P. L. Frabetti *et al.*, Phys. Rev. Lett. **72** (1994) 961;
CLEO Collaboration, K. W. Edwards *et al.*, Phys. Rev. Lett. **74** (1995) 3331.
- [23] B. Moussallam and D. Kalafatis, Phys. Lett. **B272** (1991) 196; B. Moussallam, Ann. Phys. **225** (1993) 264.
- [24] D. O. Riska and N. N. Scoccola, Phys. Lett. **B299** (1993) 338.
- [25] DELPHI Collaboration, M. Feindt *et al.*, preprint DELPHI 95-107 PHYS 542, paper submitted to the “EPS-HEP 95” Conference, Brussels, 1995;
DELPHI Collaboration, P. Abreu *et al.*, CERN preprint, CERN-PPE/96-016.

[26] Y. Oh, B.-Y. Park, and D.-P. Min, Work in progress.

[27] A. R. Edmonds, *Angular Momentum in Quantum Mechanics*, 2nd ed. (Princeton University Press, Princeton, 1974).